QUANTIFYING THE ENVIRONMENTAL AND HEALTH IMPACTS OF CURBSIDE MANAGEMENT FOR EMERGING MULTIMODAL MOBILITY SERVICES

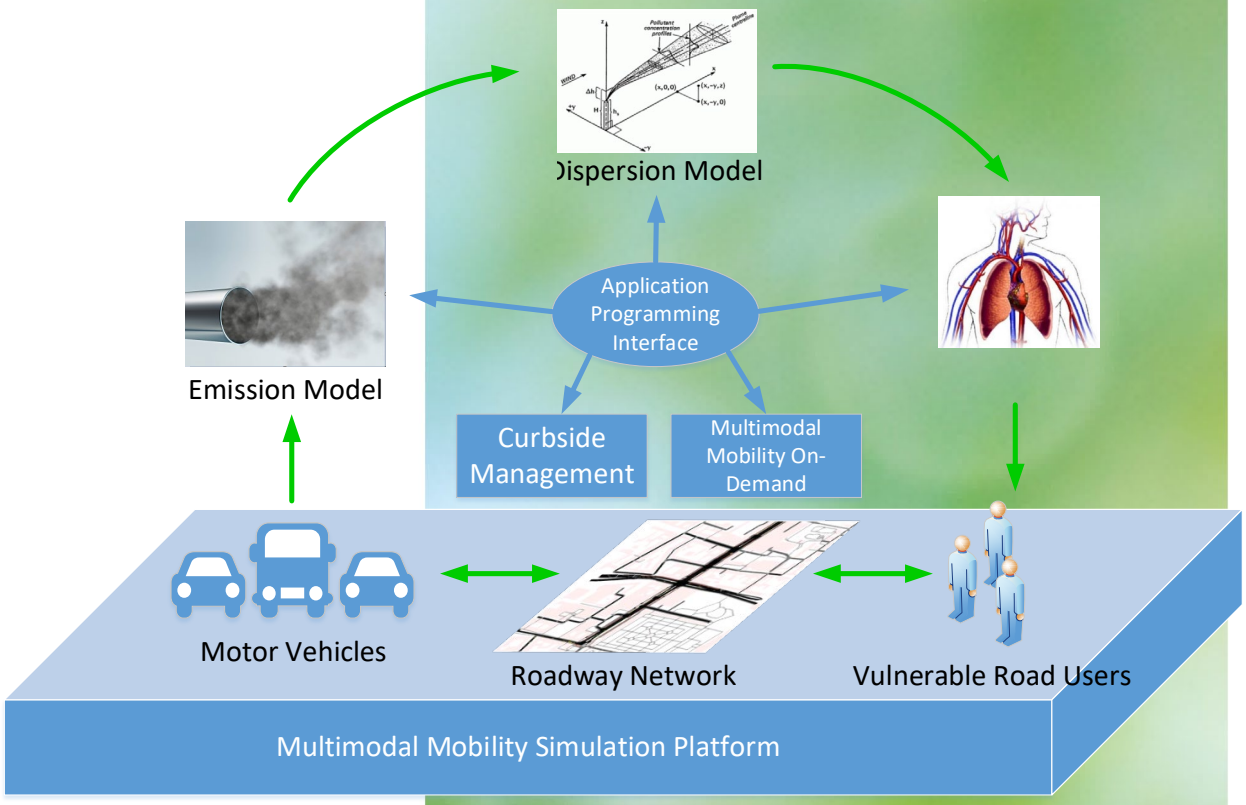

June 2022

CARTEEH

Center for Advancing Research in
Transportation Emissions, Energy, and Health
A USDOT University Transportation Center

Texas A&M Transportation Institute | Georgia Tech College of Engineering | Johns Hopkins Bloomberg School of Public Health | College of Engineering The University of Texas at El Paso | UC Riverside CE-CERT

Disclaimer

TECHNICAL REPORT DOCUMENTATION PAGE

1. Report No.	2. Government Accession No.	3. Recipient's Catalog No.
4. Title and Subtitle Quantifying the Environmental and Health Impacts of Curbside Management for Emerging Multimodal Mobility Services		5. Report Date June 2022 6. Performing Organization Code
7. Author(s) Guoyuan Wu, Xuanpeng Zhao, Peng Hao, Ji Luo, and Yifan Ding		8. Performing Organization Report No. 05-49-UCR
9. Performing Organization Name and Address: CARTEEH UTC Center for Environmental Research and Technology College of Engineering University of California, Riverside		10. Work Unit No. 11. Contract or Grant No. 69A3551747128
12. Sponsoring Agency Name and Address Office of the Secretary of Transportation (OST) U.S. Department of Transportation (USDOT)		13. Type of Report and Period Final February 1, 2021–June 30, 2022 14. Sponsoring Agency Code

15. Supplementary Notes

This project was funded by the Center for Advancing Research in Transportation Emission, Energy, and Health University Transportation Center, a grant from the U.S. Department of Transportation Office of the Assistant Secretary for Research and Technology, University Transportation Centers Program.

16. Abstract

Increasing transportation-related activities, including emerging multimodal mobility on-demand (M^3OD) services, have raised public concerns about roadway traffic and curbside management. However, most existing studies have focused on reducing traffic congestion or improving pickup and drop-off efficiency. Much less attention has been paid to air quality and human exposure. To address these gaps, we developed an integrated simulation platform capable of quantifying the environmental and health impacts at the microscopic level, such as instantaneous pollutant concentration and inhale mass per pedestrian. This innovative platform consists of five key modules: 1) Simulation of Urban Mobility for microscopic traffic modeling, 2) Motor Vehicle Emission Simulator for microscopic emission modeling, 3) a grid-based point-source dispersion model where the parameters have been calibrated by real-world measurements, 4) a MATLAB-based concentration visualizer displaying the network-wise concentration along with the simulation run, and 5) a human exposure model to estimate the instantaneous or accumulative inhale mass of target pollutants. In addition, we conducted a case study on M^3OD services with different pickup strategies. Results showed that for the scenario where everyone is picked up at the same location, human exposures to target pollutants (both nitrogen oxides and fine particulate matter in this study) were 70 and 82 percent (on average), respectively, higher than those in the scenario where pickup locations are distributed. The proposed traffic-health integrated analysis, modeling, and simulation platform can provide the quantitative results of traffic-related air quality and health impacts, and the platform is very useful for evaluating the potential environmental issues for various transportation systems management and operations strategies.

17. Key Words	18. Distribution Statement
Microscopic Traffic Simulation, Tailpipe Emission, Dispersion Modeling, Air Quality	No restrictions. This document is available to the public through the CARTEEH UTC website. http://carteeh.org

19. Security Classif. (of this report)	20. Security Classif. (of this page)	21. No. of Pages	22. Price
Unclassified	Unclassified	35	$0.00

Form DOT F 1700.7 (8-72) Reproduction of completed page authorized

Executive Summary

Increased transportation-related activity continues to have significant impacts on safety, mobility, and sustainability, thus raising a significant amount of awareness and concern from the general public. To address these issues, a variety of emerging mobility technologies and services, such as connected and automated vehicles, smart infrastructure, and shared mobility, have been developed and deployed over the past decade. Among others, multimodal mobility on demand (M^3OD) services such as ride hailing have not only unlocked novel opportunities for urban transportation but also introduced new challenges to users, service providers, and public transportation agencies alike. However, very little research related to M^3OD services has focused on environmental and health impacts.

To address this issue, the research team developed an integrated simulation platform that is capable of modeling and analyzing the environmental and health impacts of emerging mobility technologies and services (including M^3OD) at the microscopic level, such as instantaneous pollutant concentration and inhale mass per pedestrian. The five key modules in this innovative platform are:

1. Simulation of Urban Mobility (SUMO) for microscopic traffic modeling.
2. Motor Vehicle Emission Simulator (MOVES) for microscopic emission modeling.
3. A grid-based point-source dispersion model where the parameters have been calibrated by real-world measurements.
4. A MATLAB-based concentration visualizer displaying the network-wise concentration along with the simulation run.
5. A human exposure model to estimate instantaneous or accumulative inhale mass of target pollutants.

Case studies were performed on M^3OD services along a roadway network in Riverside, California, with different curbside management strategies. Results indicated that for the scenario(s) where all pickups and drop-offs happen at the same location, human exposures to target pollutants (e.g., nitrogen oxides and particulate matter 2.5 microns or less in diameter) can be around 70 and 82 percent (on average), respectively, higher than those in the scenario where pickup/drop-off locations are distributed.

In terms of the project impacts, the proposed traffic-health integrated analysis, modeling, and simulation platform can provide the quantitative results of traffic-related air quality and health impacts, due to the introduction of emerging transportation technologies and services. The platform can be a very useful tool for decision makers to evaluate the potential environmental issues or environmental justice of various transportation systems management and operations strategies.

Acknowledgments

This research, project 05-49-UCR, was funded by the Center for Advancing Research in Transportation Emission, Energy, and Health (CARTEEH). The authors would like to thank Dr. Akula Venkatram and Dr. Kanok Boriboonsomsin for the support of field data collection and insightful discussion. The authors also acknowledge the California Air Resource Board for providing a portable emission acquisition system to measure carbon dioxide concentration, and valuable feedback from Dr. Shaohua Hu.

Table of Contents

List of Figures

List of Tables

Introduction

CARTEEH QUICK FACTS

CARTEEH is a Tier 1 University Transportation Center, funded by the U.S. Department of Transportation's Office of the Secretary for Research and Technology.

Environmental sustainability is one of the critical performance measures in the field of transportation. In recent years, increased transportation-related activities have raised awareness and concerns from the general public about air pollution and health impacts. In 2018, the transportation sector was the largest producer of greenhouse gases (GHGs) nationwide, accounting for approximately 28.2 percent of total U.S. GHG emission [1]. To address these issues, a variety of emerging mobility technologies and services, such as connected and automated vehicles (CAVs), smart infrastructure, and shared mobility, have been developed and deployed over the past decade [2]. For example, CAV technology has been widely studied to improve the sustainability of transportation systems, where a CAV can be driven by itself with the help of its onboard perception sensors and can communicate with the other equipped vehicles (through vehicle-to-vehicle communications), roadside infrastructure (through vehicle-to-infrastructure communications), and the cloud [3]. Representative applications for urban scenarios are eco-approach and departure [4, 5]. Besides the advanced technologies on the vehicle side, some researchers focus on the infrastructure side to improve the overall energy efficiency of the traffic system. Lee et al. [6] proposed a cooperative vehicle intersection control system that enables cooperation between vehicles and infrastructure for effective intersection operation and management, thus enhancing system throughput and environmental sustainability.

In addition to the advances on both the vehicle and infrastructure sides, emerging multimodal mobility on-demand (M^3OD) services such as micro-mobility and ride hailing have not only unlocked novel opportunities for urban transportation but also introduced new challenges to users, service providers, and public transportation agencies alike. For example, the increased curbside activities due to the prevalence of multimodal mobility as a service have not only created congestion for the traffic of different modes along curbs or on sidewalks, but have also formed potential bottlenecks that may affect the upstream on-road vehicular flows. From an environmental perspective, traffic congestion near the curbside would lead to additional environment concerns such as energy waste and excessive tailpipe emission, thus forming hotspot(s) with highly concentrated pollutants. Even worse, due to the high-volume pedestrian and/or other nonmotorized traffic on the sidewalks, much more safety risks will be raised, and detrimental health impacts would be imposed on those vulnerable road users. Most of the research related to these emerging M^3OD services has focused on accessibility, safety, and congestion impacts, but much less attention has been raised from the perspective of their resultant environmental and health impacts. In particular, how well-designed curbside management strategies would affect the roadway traffic (vehicular) and sidewalk traffic (pedestrian or other micro-mobility) is still an open research question. In addition, how these strategies would influence the air quality and vulnerable road users' exposure to motor vehicular pollutants and mobile source air toxics is a critical concern for local governments (e.g., cities and metropolitan planning organizations), especially for disadvantage communities.

To address the aforementioned gaps, this study developed an integrated simulation platform (as shown in Figure 1), which is able to:

- Model a multimodal transportation system with high resolution, including the roadway network, motorized vehicles (e.g., passenger cars, trucks, and shuttles), and nonmotorized transportation modes (e.g., pedestrians, bicyclists, or even other micro-mobility travelers).
- Model the traffic-related pollutant emission, which may include tailpipe emission and even brake/tire worn emission.
- Model the traffic-related air quality dispersion.
- Model the potential health impacts (i.e., exposure to those vulnerable road users).

- Implement different curbside management strategies in response to M^{3}OD services.
- Evaluate the system performance especially in terms of environmental footprints and health impacts.

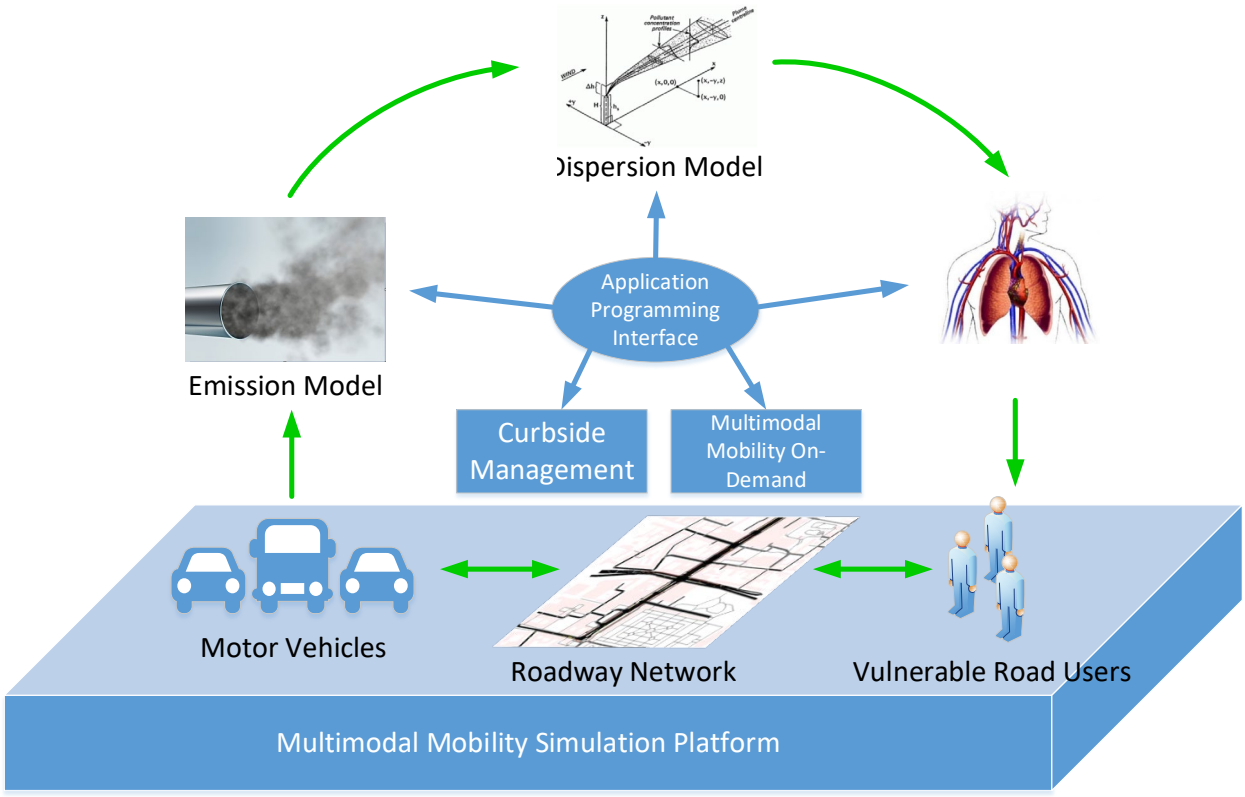

Figure 1. Concept of integrated modeling for quantifying the environmental and health impacts related to M^{3}OD transportation services.

The rest of this paper is organized as follows:

- The next section reviews the existing literature related to microscopic traffic simulators, vehicular emission models, tailpipe pollutant dispersion models, and their applications to urban traffic scenarios.
- Major efforts in developing the integrated modeling platform in Simulation of Urban Mobility (SUMO) are presented in the third section, where each module is elaborated upon.
- Based on the real-world network in the city of Riverside, the fourth section describes a case study on M^{3}OD services and provides the quantitative results of tailpipe emission and human exposure for different curbside management strategies.
- The last section concludes this study with potential improvements for future research.

Literature Review

Microscopic Traffic Simulators

Currently, several microscopic simulators are available to support modeling traffic scenarios in a realistic manner, including the roadway network, motor vehicles, and nonmotorized road users (e.g., pedestrians and bicyclists). Among them, PTV VISSIM [7] and Aimsun [8] are two major commercial simulation tools. Specifically, VISSIM is a behavior-based multi-purpose microscopic simulation that can be linked with MATLAB through the Component Object Model interface or with C/C++ via dedicated application programming interfaces (APIs). Aimsun is a hybrid traffic modeling simulator that allows simultaneous application of multimodal analysis with large networks. On the

other hand, SUMO [9] is an open-source traffic simulator that has been widely used for a variety of applications, such as dynamic navigation, traffic surveillance systems evaluation, and traffic light algorithm development [10]. In addition, SUMO provides APIs, called Traffic Control Interface (TraCI), to facilitate the interaction with external applications through a socket (bidirectional) connection. SUMO also includes a few emission models, such as the Handbook Emission Factors for Road Transport (HBEFA) and Passenger Car and Heavy-Duty Emission Model developed for the European vehicle fleet.

Vehicular Emission Models

Vehicular emission models estimate the emission rates and/or emission factors of motorized vehicles based on different traffic conditions and driving cycles. The models can be classified into three main types:

- Microscopic.
- Macroscopic.
- Average velocity-based statistic.

In this study, we mainly focused on the microscopic models derived from the relationship between the second-by-second vehicle trajectories and emission rates. The Comprehensive Modal Emission Model can predict second-by-second tailpipe emission and fuel consumption based on different modal operations from the in-use vehicle fleet [11]. The calculation method fully considers the power and speed of the engine to accurately reflect the emission characteristics of the vehicle, which belongs to transient physical models. Another well-accepted model is the Virginia Tech microscopic model that was developed using chassis dynamometer data on light-duty vehicles and trucks [12]. A polynomial regression model on key vehicle dynamics, such as speed, acceleration, and power, is set up to estimate non-steady-state emission. As aforementioned, HBEFA is adopted in SUMO and is widely used for fleets in European countries [13]. Based on traffic activities, HBEFA can provide emission factors by:

- Type of emission (e.g., hot run or cold start).
- Vehicle category (e.g., passenger cars, heavy-duty vehicles, or buses).
- Year (1990–2050 for most countries).
- Pollutants including carbon monoxide, hydrocarbons, nitrogen oxides (NOx), particulate matter (PM), carbon dioxide (CO_2), ammonia, and nitrous oxide.

Over the past decade, the U.S. Environmental Protection Agency (EPA) has been developing a state-of-the-art vehicular emission model, called Motor Vehicle Emission Simulator (MOVES) [14]. By applying the binning strategy, MOVES aims to estimate vehicular emission at multiple scales: microscopic (for individual vehicles), mesoscopic (based on link-level traffic data), and macroscopic (i.e., aggregated inventory for a region or even the entire nation). The open database and model structure of MOVES increases its transferability, allowing other stakeholders to collect their own datasets that represent local traffic conditions, vehicle mix, and driving trajectories to estimate the specific tailpipe emission inventory. In particular, the open database in MOVES stores the base emission rates of different criteria pollutants for different vehicle types, vehicle ages, and operating mode bins (depending on speed, acceleration, and vehicle specific power).

Dispersion Models and Their Applications

A large number of dispersion models have been developed for estimating the concentration of air pollutants. These models can be classified into different categories from different perspectives. In terms of modeling mechanism, there are *Gaussian models*, *box models*, *Lagrangian models*, and *computational fluid dynamics (CFD) models* [15]. Based on the emission source type, the dispersion models can be categorized into point-source models, line-source models, area source models, and volume source models. For example, the CALPUFF model can simulate the dispersion effects of point, line, area, or volume sources with spatiotemporally varying meteorological conditions, based on similarity equations. The CALPUFF model generally exhibits good results in the validation

experiments but is not suitable for modeling the scenarios with time scales less than 1 hour or in an urban environment [16]. Another widely used model is AERMOD, which is a steady-state Gaussian plume model [17]. By assuming both vertical and horizontal concentration distributions to be Gaussian, AERMOD can handle flows in complex terrains using the dividing streamline concept. Similar to that of CALPUFF, the modeling time span of AERMOD should not be less than 1 hour.

In recent years, a few studies have focused on the application of dispersion models to urban scenarios to evaluate the impacts of different traffic management strategies. Lefebvre et al. [18] presented an integrated model framework consisting of an advanced measurement interpolation model, a bi-Gaussian plume model, and a canyon model to simulate the urban traffic scenario at the street level. Shi et al. [19] leveraged a CFD-based model to simulate scenarios with street canyons and visualize the exhaust emission of moving vehicles using dynamic mesh updating method, which could even capture the vehicle-movement-induced turbulence effects. Besides urban street scenarios, Damoiseaux and Schutter [20] developed a line-source Gaussian puff (LSGP) model capable of estimating distributions of gaseous pollutants in the vicinity of a freeway and applied the model to assessing real-time traffic control, such as a variable speed limit. Nevertheless, LSGP is not suitable for microscopic simulation (at the individual vehicle level) because it is a line-source model. Zegeye [21] proposed a computationally efficient point-source dispersion model, which could update the pollutant concentration on a grid basis. This model requires trivial computational loads, which makes it suitable for online estimation of environmental impacts due to traffic management at a microscopic level.

Integrated Modeling Platform

In this study, we leveraged the capacity of SUMO and built up an integrated modeling platform (as depicted in Figure 1) by adding other key modules, including MOVES, a grid-based dispersion model, a human exposure model, a MATLAB-based concentration visualizer, and heuristic strategies for M^3OD services (via TraCI).

Workflow

Figure 2 presents the workflow developed for the modeling platform to quantify the environmental and health impacts related to M^3OD services. As illustrated in the figure, we first created a multimodal traffic network in SUMO, including taxis or Uber/Lyft vehicles, background traffic (i.e., passenger vehicles), and pedestrians waiting for services. Then, the second-by-second vehicular tailpipe emission were estimated by the coded MOVES model. With the developed dispersion module, grid-wise pollutant concentrations were estimated based on both emission and meteorological conditions. The results can be visualized online through a custom-built visualization tool using MATLAB. The instant and accumulative exposure to specific pollutant (e.g., NOx and PM) for each individual vulnerable road user can be estimated, depending on the user's instant location (i.e., in which grid at each time step) and trajectory as well as gender-/age-related characteristics (e.g., height and breathing rate).

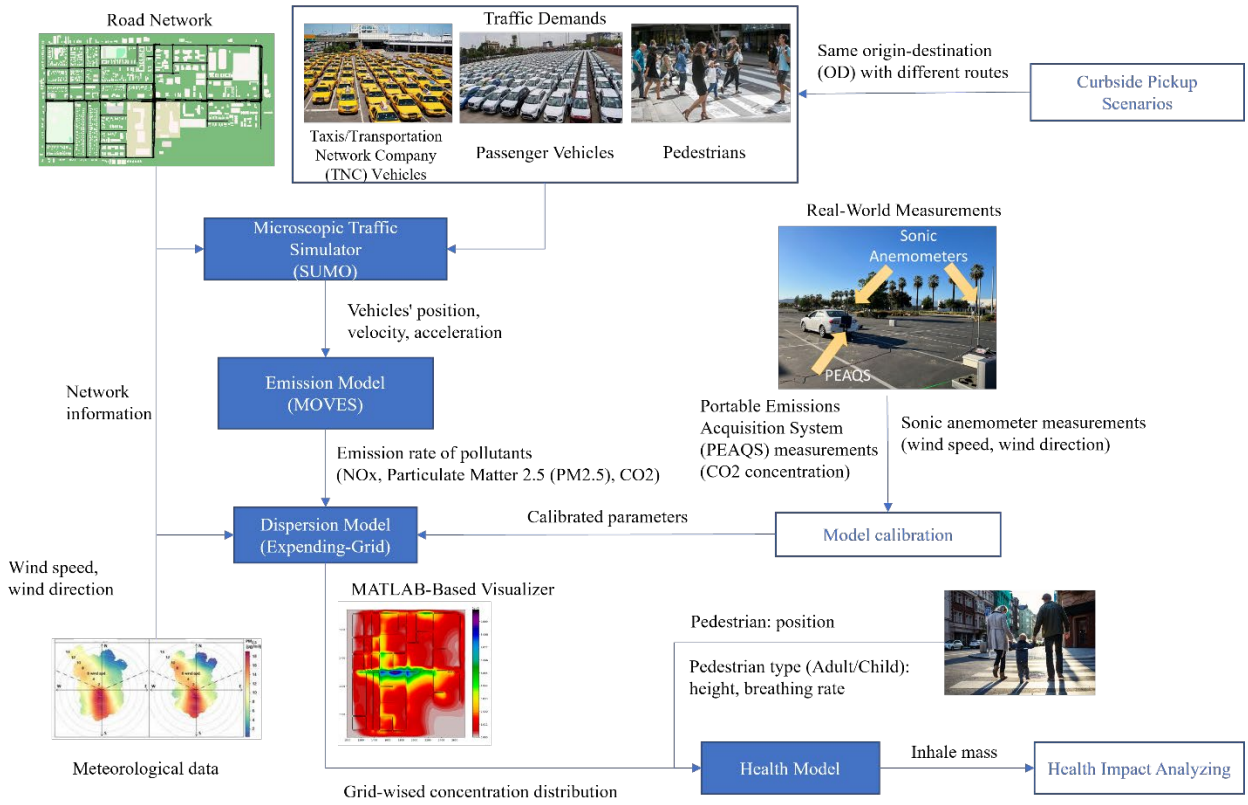

Figure 2. Workflow to run the integrated modeling platform.

Key Module 1—Simulation of Urban Mobility

SUMO not only serves as a microscopic traffic simulator but also provides powerful APIs to extend its capability. For example, OsmWebWizard.py can select the real-world region from the Open Steet Map to generate the target simulation network without laborious efforts. RandomTrips.py can generate a set of random trips in a given network that would apply to both vehicles and pedestrians. More information about the functionalities of SUMO is available at https://www.eclipse.org/sumo/.

Key Module 2—Motor Vehicle Emission Simulator

The original MOVES model developed by EPA is very comprehensive and not suitable for online interaction with microscopic traffic simulation. In this study, we developed an alternative approach to simplify the application of MOVES to simulation while keeping reasonable fidelity similar to the original MOVES model. Figure 3 depicts the workflow of MOVES plug-in development for SUMO. Similar procedures can be applied to the development of other microscopic simulation tools (e.g., VISSIM). Two major procedures are:

- Acquiring emission rate tables from MOVES.
- Developing the operating mode for each vehicle at each time step in the simulation.

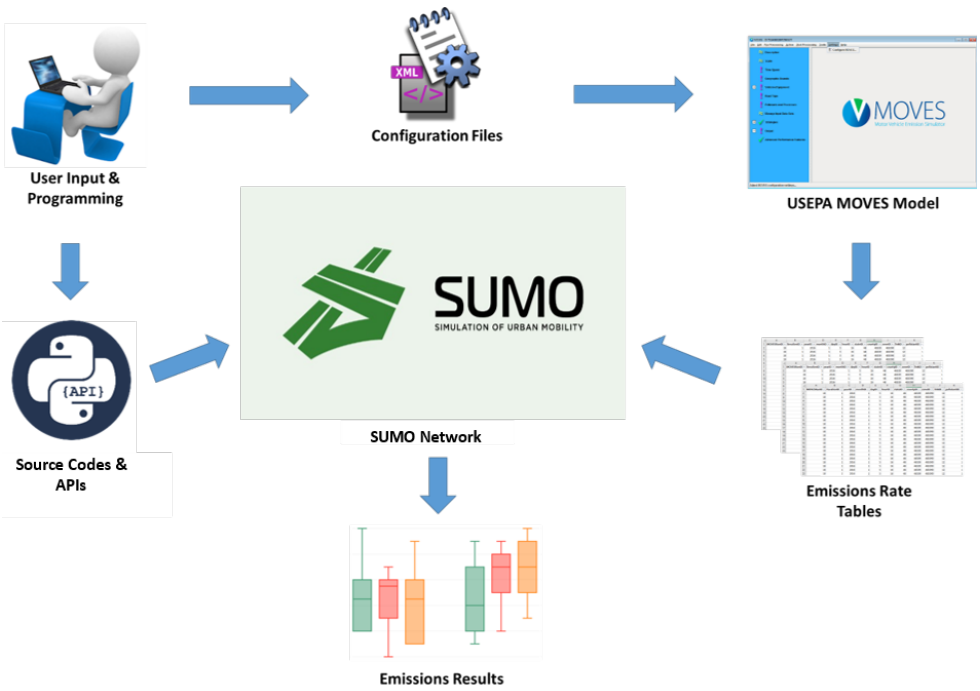

Figure 3. Workflow for developing a MOVES plug-in in SUMO.

Acquiring Emission Rate Tables from MOVES

To retrieve the customized emission rate tables (from MOVES), we first inputted the network model information into the MOVES model, such as geographic region (e.g., Riverside, California) and the calendar month and year to be modeled (e.g., June 2022). In the meantime, we prepared a set of configuration files that could be linked to the MOVES database, including vehicle population/activity, fuel type/engine technology, vehicle inspection/maintenance program, and meteorological statistics. Once all the input data files were ready, MOVES was executed and outputted emission rate tables for different source types (e.g., passenger car or truck), considering various factors, such as vehicle model year distribution, fuel type/engine technology market share, and temperature and/or humidity adjustment.

Developing Code to Calculate Operating Mode in Simulation

In SUMO, TraCI can access second-by-second vehicle trajectories (including both speeds and accelerations) and road grade (if any). With this activity data for each vehicle and roadway geometry, as well as the information on vehicle class and weight, the vehicle specific power (VSP) characteristics (in kWatt/tonne) can be calculated by [22]:

$$\boldsymbol{VSP} = \left(\boldsymbol{A}/\boldsymbol{M}\right) \cdot \boldsymbol{v} + \left(\boldsymbol{B}/\boldsymbol{M}\right) \cdot \boldsymbol{v^2} + \left(\boldsymbol{C}/\boldsymbol{M}\right) \cdot \boldsymbol{v^3} + (\boldsymbol{a} + \boldsymbol{g} \cdot \sin\boldsymbol{\theta}) \cdot \boldsymbol{v} \quad (1)$$

where A, B, and C are the road-load-related coefficients for rolling resistance ($\mathrm{kW} \cdot \mathrm{sec/m}$), rotating resistance ($\mathrm{kW} \cdot \mathrm{sec^2/m^2}$), and aerodynamic drag ($\mathrm{kW} \cdot \mathrm{sec^3/m^3}$), respectively; v is the vehicle speed ($\mathrm{m/sec}$); M is the mass of the vehicle (metric ton); g is the acceleration due to gravity ($9.8\ \mathrm{m/sec^2}$); a is the vehicle acceleration (meter/sec2); and θ is the (fractional) road grade. EPA provides the default values of these parameters [22]. After the VSP values were calculated, they were binned according to the MOVES vehicle operating mode bin definition given by Wang et al. [23], as shown in Figure 4. With the emission rate tables coded in SUMO, the energy consumption and pollutant emission could be estimated in either disaggregate (e.g., second by second for each vehicle) or aggregate in the spatiotemporal manner.

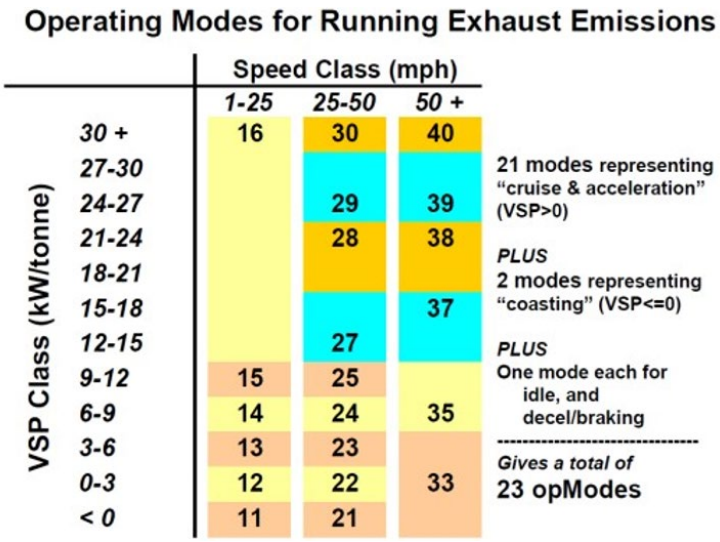

Figure 4. Operating mode binning scheme in MOVES.

(From: Wang, Z., Wu, G., Scora, G., 2021. MOVESTAR: An Open-Source Vehicle Fuel and Emission Model based on USEPA MOVES.)

Key Module 3—Grid-Based Dispersion Model

Key Idea

Inspired by Zegeye's work [21], we developed a semi-three-dimensional (3D) grid-based dispersion model that requires little computational power and can be implemented in microscopic traffic simulation for online application. The developed model divides the area of interest into a set of square grids and updates the pollutant concentration in each grid at every time step. The process of the model mainly consists of two steps:

1. Adding new emission source(s) into grid(s).
2. Diffusing the existing emission.

In the first step, every emission source is regarded as a point source in a two-dimensional Cartesian coordinate system denoted by (x_i, y_i). Based on the output from the MOVES model, the concentration of a new source i can be derived from:

$$conc\ (x_i^c, y_i^c, k+1) = conc(x_i^c, y_i^c, k) + er_i(k) * \Delta t/A \quad (2)$$

where $conc(x_i^c, y_i^c, k)$ is the concentration of grid (x_i^c, y_i^c) at time step k, (x_i^c, y_i^c) are the grid center coordinates associated with the position of the point source located at (x_i, y_i), $er_i(k)$ is the emission rate of the point source i at time step k, Δt is the time step length, and A is the area of grid (x_i^c, y_i^c) that equals to the square of the side length L of grid (x_i^c, y_i^c).

The diffusing step considers two processes: expanding and evaporating. Expanding takes care of the dispersion along the horizontal plane, while evaporating accounts for the dispersion along the vertical axis. Specifically, we considered the expanding process under two scenarios: with wind and without wind. When there is no wind, it is assumed that emission expand in all directions uniformly, as illustrated in Figure 5(a), and

$$L_e = (1 + \Delta t\omega)L \quad (3)$$

where $L_e$is the side length of the expanded emission puff and ω is the expansion factor of the emission (to be calibrated). When the wind speed is not zero, the emission expands toward the wind direction as shown in

Figure 5(b), where V_w stands for the wind speed. Then, we can calculate the concentration of the neighbors' grids of the point source in the next time step according to the following equation:

$$conc(x_i^n, y_i^n, k+1) = \frac{\alpha^{(x_i^n, y_i^n)}_{(x_i^c, y_i^c)}}{L_e^2} * conc(x_i^c, y_i^c, k) + conc(x_i^n, y_i^n, k) \quad (4)$$

where $conc(x_i^n, y_i^n, k)$ is the concentration of neighbor grids with respect to grid (x_i^c, y_i^c) at time step k; $(x_i^n, y_i^n) \in \mathcal{N}(x_i^c, y_i^c)$, $\mathcal{N}(x_i^c, y_i^c)$ is the set of neighbor grids with respect to grid (x_i^c, y_i^c), which is $\{(x_i^{c-1}, y_i^{c-1}), (x_i^c, y_i^{c-1}), (x_i^{c+1}, y_i^c), (x_i^{c-1}, y_i^c), (x_i^{c+1}, y_i^c), (x_i^{c-1}, y_i^{c+1}), (x_i^c, y_i^{c+1}), (x_i^{c+1}, y_i^{c+1})\}$; and $\alpha^{(x_i^n, y_i^n)}_{(x_i^c, y_i^c)}$ is the expanded area from the source grid (x_i^c, y_i^c) to the target grid (x_i^n, y_i^n). For example, $\alpha^{(x_i^{c-1}, y_i^{c+1})}_{(x_i^c, y_i^c)}$ is highlighted as in Figure 5(a).

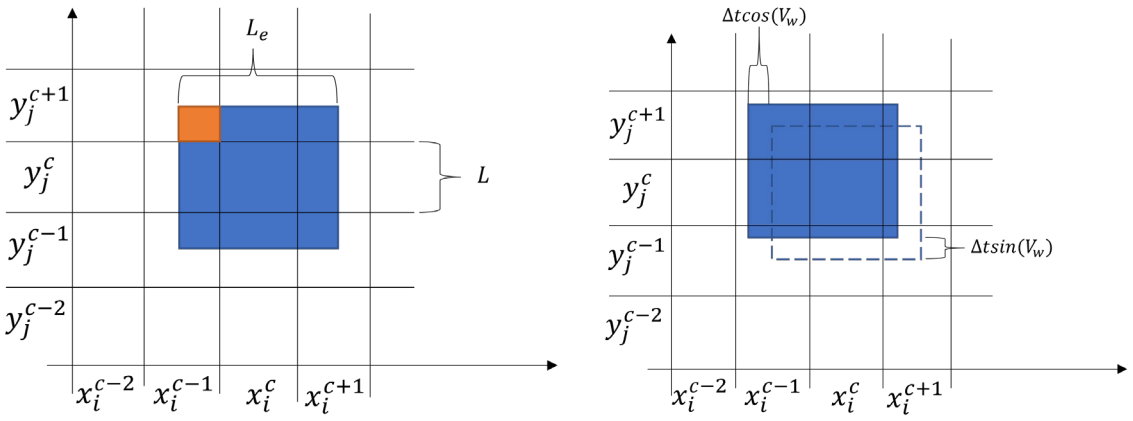

(a) Without wind (b) With wind

Figure 5. Illustration of the expanding mechanism under two scenarios.

Besides the expanding mechanism, the evaporating process characterizes the vertical emission diffusion (or escaping). For simplicity, an evaporating factor $\gamma \in (0, 1)$ (to be calibrated) is applied:

$$conc(x^a, y^a, k+1) = conc(x^a, y^a, k) * (1-\gamma) \quad (5)$$

where grid (x^a, y^a) refers to any grid in the concentration matrix. Therefore, the concentration $conc(x^a, y^a, k+1)$ of grid (x^a, y^a) along the horizontal plane at time step $k+1$ is given by

$$conc(x^a, y^a, k+1) = [\sum_{\{i:(x_i^c, y_i^c)=(x^a, y^a)\}} er_i(k) * \frac{\Delta t}{A}$$

$$+ \sum_{(x_i^n, y_i^n) \in \mathcal{N}(x^a, y^a)} \frac{\alpha^{(x^a, y^a)}_{(x_i^n, y_i^n)}}{L_e^2} * conc(x_i^n, y_i^n, k)] * (1-\gamma) \quad (6)$$

However, these equations can only model the two-dimensional dispersion because it assumes the emission source and the measurements receptor are on the same horizontal plane. This assumption does not hold for most of the transportation applications. Generally, the major emission source of a motor vehicle is located at the tailpipe (e.g., around 0.3 m above the ground), but the height of a receptor (e.g., pedestrian) may vary when investigating the

human exposure or health effects. To address this issue, we proposed a simplified solution by introducing a decay function to characterize the diffusion along the vertical axis:

$$er_i^r = \exp\left(-\frac{(h_r-h_s)^2}{2*\sigma^2}\right) * er_i^s \quad (7)$$

where h_s and h_r are the height of the emission source and the height of the receptor, respectively; er_i^s is the emission rate of the i-th point source (with respect to the height of the source); er_i^r is the equivalent decayed emission rate if the emission source is at the same height of the receptor; and σ is the decay factor (to be calibrated).

Field Data Collection

To calibrate the three factors used in the dispersion model, we conducted a field experiment in the parking lot of the College of Engineering Center for Environmental Research and Technology at the University of California, Riverside [24]. The location is far enough from roads to avoid contamination of the CO_2 measurements by emission from vehicles traveling on these roads. A 2012 Toyota Corolla LE model with a 1.8-liter internal combustion engine served as the source of emission. The exhaust tailpipe was 26 cm above the ground. Figure 6 shows the experimental setup, and a polar coordinate system for measurements was used in this study. The concentrations were collected at a radius of 1, 2, 3, and 4 m centered around the tailpipe at angles of 30°, 60°, 90°, 120°, and 150° and at heights of 0.3, 0.6, and 1.2 m above the ground.

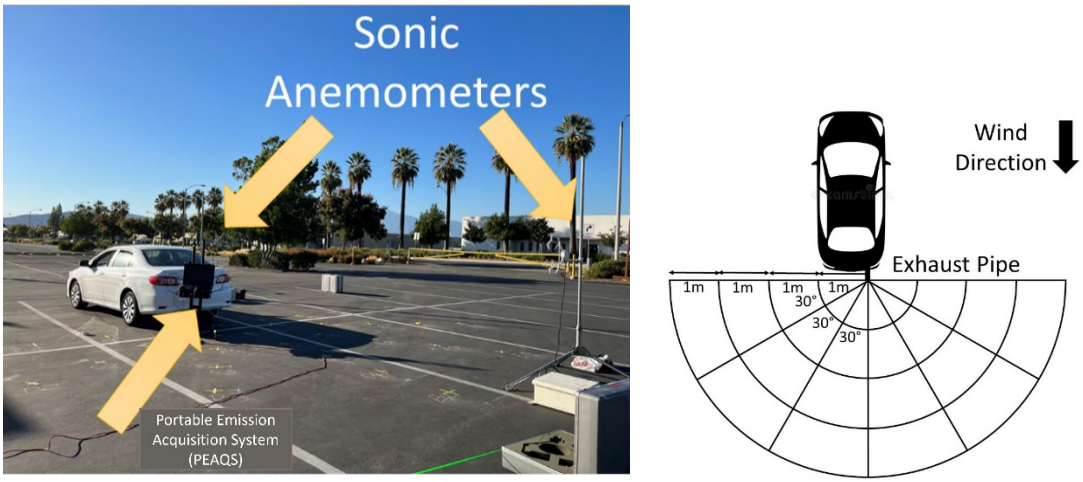

Figure 6. Experimental layout showing instruments used in the study.

The meteorological data were collected using two CSAT3 3D sonic anemometers mounted at a height of 1.5 m with a frequency of 20 Hz. One sonic anemometer (Figure 6) was placed west (upwind) of the vehicle, and the other was placed east (downwind) of the vehicle to measure the turbulence effects caused by the vehicle. Figure 7 shows the 5-minute averaged meteorological data. The experiment was conducted in two shifts. During daytime, a stable west wind blew from the front to the back of the vehicle; during nighttime, the wind direction shifted more frequently. In addition, as indicated by the red dots in the figure, the surface friction velocities u_* during nighttime were around half of the values measured during daytime.

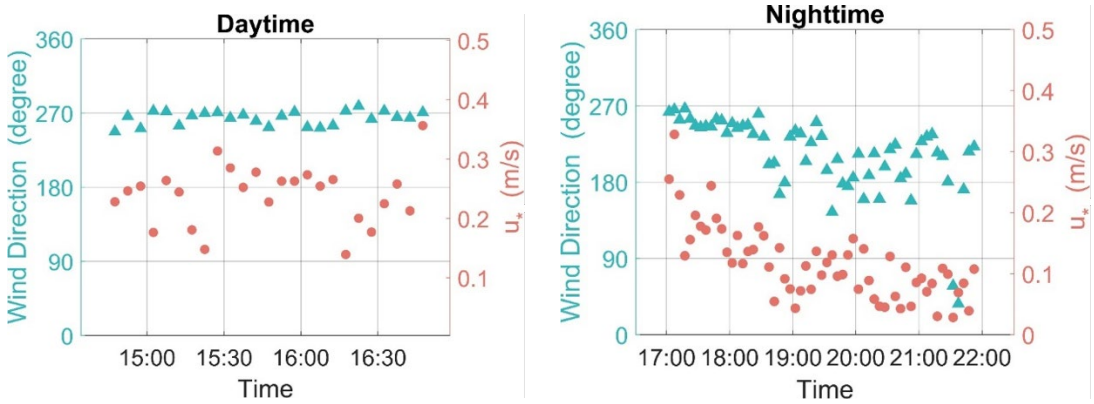

Figure 7. Wind direction and surface friction velocities u_* from downwind sonic anemometer averaging every 5 minutes.

The tailpipe temperature was sampled instantaneously for each measurement using an infrared thermometer. Figure 8 shows the variation of temperature of the exhaust gases during the two cycles (one is called "idling," while the other is called "power") used in the field study. Based on the measurements, the tailpipe temperature during idling was about 60°C, the tailpipe temperature during the power cycle exceeded 175°C, and the ambient temperature was approximately 20°C.

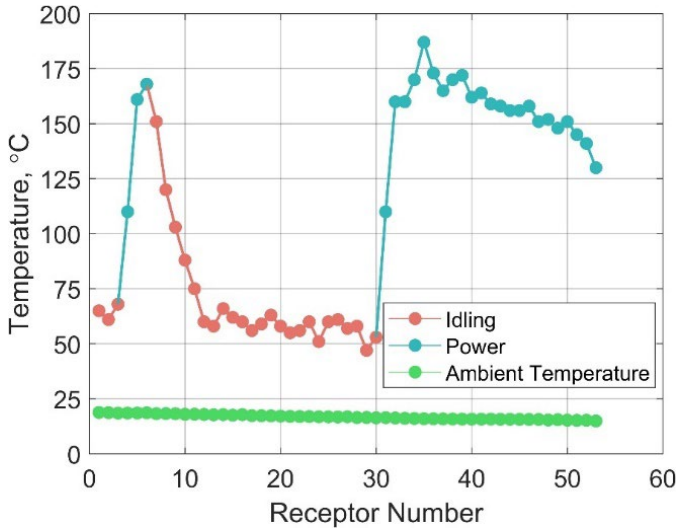

Figure 8. Variation of tailpipe temperature and ambient temperature under different vehicle conditions.

We used CO_2 as the tracer of emission from the tailpipe because the concentration close to the vehicle tailpipe was well above the background concentration of 415 ppm. CO_2 concentration was measured at several distances and heights from the source using a Portable Emission Acquisition System (PEAQS), provided by the California Air Resources Board (CARB). A PEAQS, which can make real-time concentration measurements, includes a LI-840 CO_2 gas analyzer and a low-cost single-board computer Raspberry Pi inside, as shown in Figure 9. At each location, sampling was conducted over 2 to 5 minutes to catch a stable plume signal.

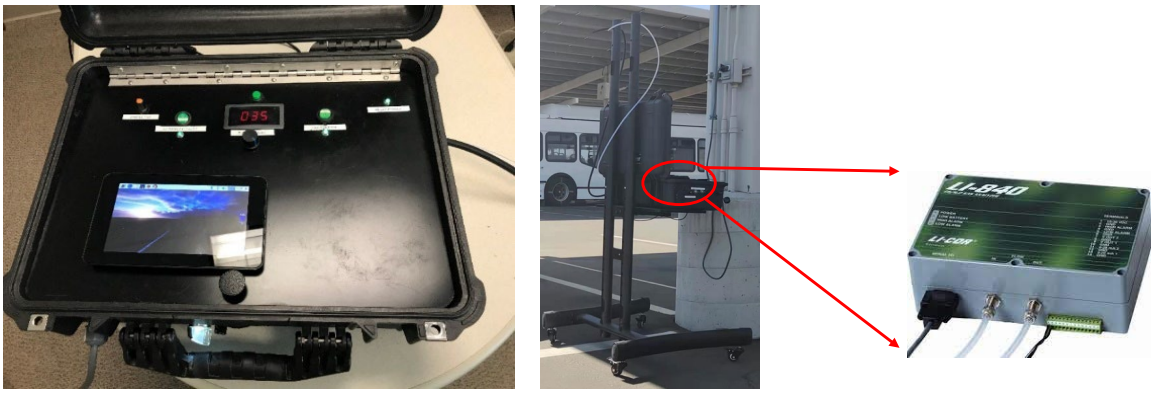

Figure 9. PEAQS developed by CARB.

An onboard diagnosis device called OBDLink MX (Figure 10) recorded the fuel consumption rate every second. The emission rates were computed from the recorded fuel consumption rates assuming complete combustion of the fuel. The gas pedal was positioned to produce two CO_2 emission rates, one during idling and the other during power. Table 1 gives the arc-averaged measured CO_2 concentrations. Because the concentrations at different heights and distances were not measured at the same time, they did not always exhibit the expected decreasing trends with increase in height and distance from the source.

Figure 10. OBDLink MX.

Table 1. Arc-Averaged CO_2 Concentrations above Background (in ppm) at Different Heights and Distances

Distance (m) \ Z (m)		Idling			Power		
		0.3	**0.6**	**1.2**	**0.3**	**0.6**	**1.2**
Daytime	1	99	—	—	242	—	—
	2	34	—	—	188	—	—
	3	11	—	4	—	—	20
Nighttime	1	358	38	16	1,224	635	118
	2	**147**	**30**	**14**	**55**	4	**68**
	3	**75**	**59**	**15**	**21**	**75**	**27**

Modeling Calibration

We set up the same configuration in the numerical simulation for calibrating the following factors: expanding factor, evaporation factor, and decay factor. A point source was placed at the center of the mesh, and the height of the mesh plane was assumed to be 0.3 m. The locations of receivers were transferred from the polar coordinate system to the Cartesian coordinate system (e.g. [1, 90°] to [1, 0]). The time step was set to be 0.1 seconds.

From the horizontal plane (at the same height of the emission source), we calibrated the expanding factor and evaporation factor first. Using the meteorological data collected by anemometers and the concentration data collected by the PEAQS as model inputs, we simulated the same process as that in the field and estimated the steady-state concentrations at the locations of receptors. The steady-state concentration in simulation was

determined when the sum of the difference of simulated concentrations between two consecutive time steps was close to zero. This was consistent with the measurements in the field experiment because we kept the emission source on for a while to ensure a steady state of plume. Then, we tuned the expanding factor and evaporation factor against real-world data by applying the least square technique. Figure 11 shows the calibrated results.

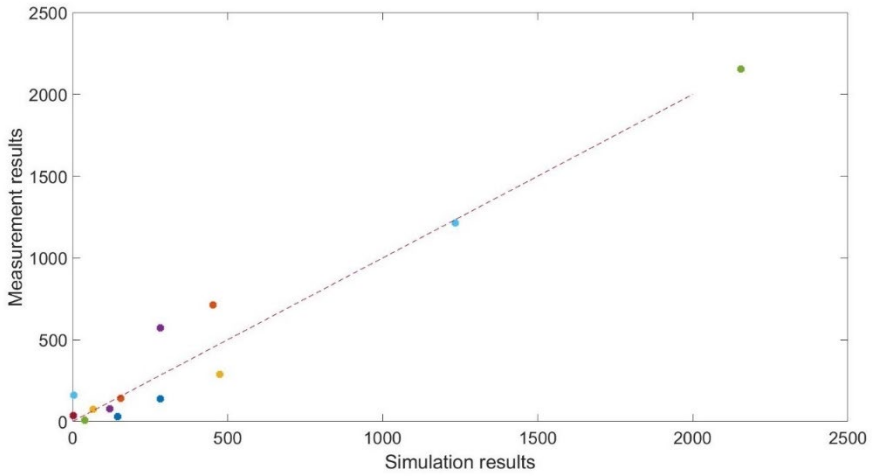

Figure 11. Simulated concentrations versus measured concentrations after calibrating the expanding factor and evaporating factor.

From the vertical perspective, the calibration of decay factor follows Equation 7. We firstly divided the concentration measurements of other planes (i.e., 0.6 and 1.2 m above the ground) by the concentration measurements of corresponding receptors at the source plane (i.e., at the height of 0.3 m). Then, we fitted our Gaussian decay function with the data points, as shown in Figure 12. We ignored the buoyancy impact and ruled out the data points whose emission rates were higher than the source plane.

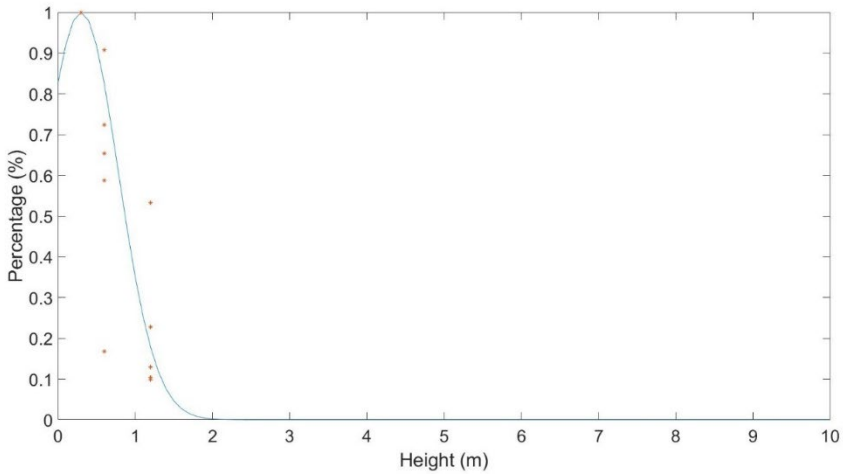

Figure 12. Calibration results for decay factor.

Key Module 4—MATLAB-Based Online Visualizer

SUMO has its own graphical user interface (GUI) showing the road network, real-time traffic, and pedestrian flows but not the emission or concentrations. In this project, we developed a MATLAB-based routine for visualizing the real-time concentration of the area of interest using a colormap, along with the simulation run in SUMO. To achieve this, we first read and displayed the road network from the net file of SUMO. Then, we created grids based on the size of the entire network and the defined grid size. The side length of the entire mesh area was extended

to be 10 percent larger than the target road network to avoid any margin problem. Finally, we displayed the concentration matrix by the "nipy_spectral" colormap. A color bar indicated the mapping of data values, and its range kept updating based on the latest concentration matrix. Figure 13 presents an example of the concentration map (overlaying the roadway network) output from the MATLAB-based Visualizer.

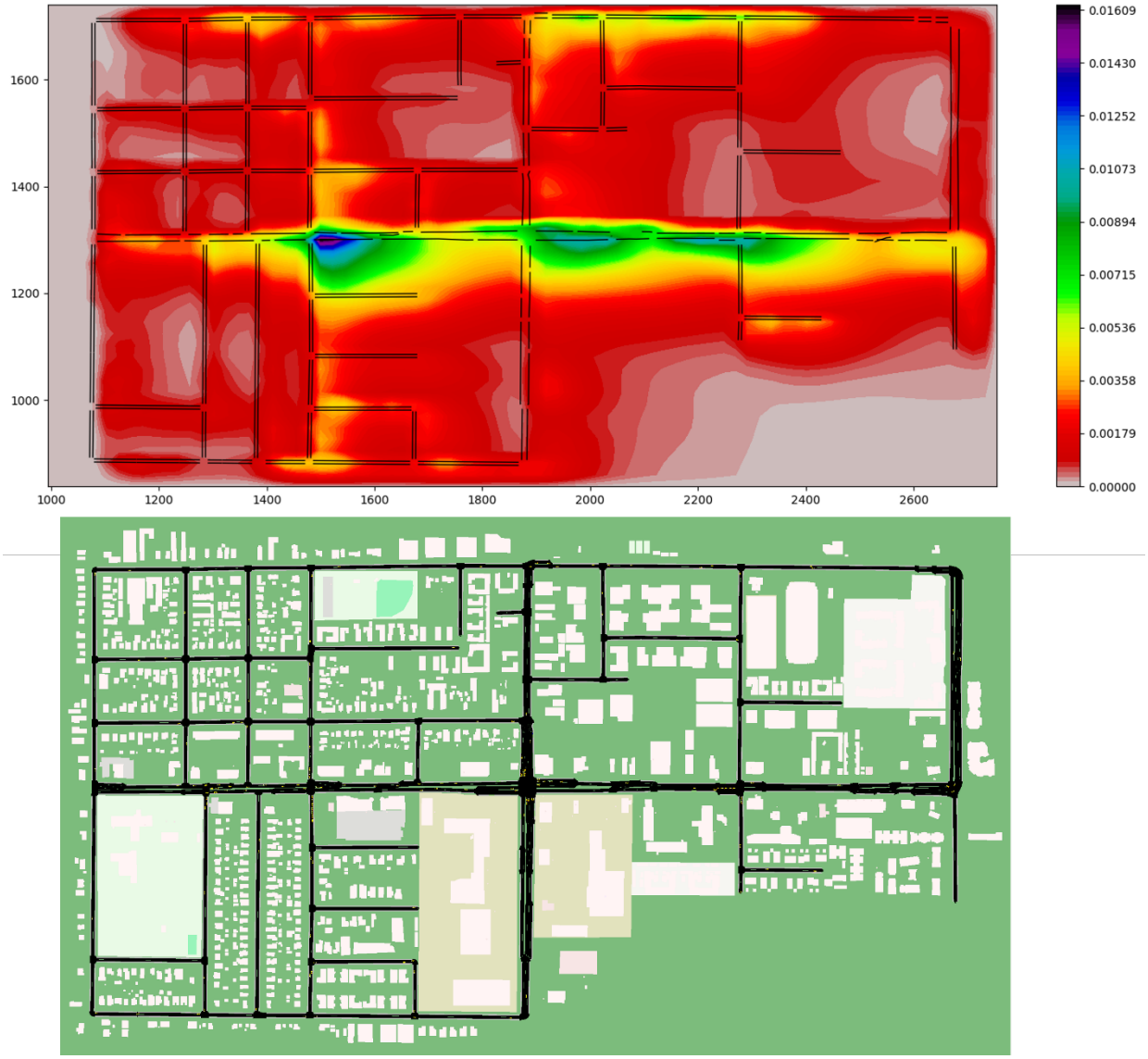

Figure 13. A screenshot of the MATLAB-based Visualizer for an example simulation run in SUMO.

Key Module 5—Human Exposure Model

In this research, human exposure is the amount of pollutant inhaled by a person subject. To assess the pollutant exposure, inhaled mass (IM) was used as the metric and was calculated by Equation 8 [25]. Assuming a pedestrian subject i is located within grid(x_{jc}, y_{jc}) at time step k, then

$$IM_i(k) = conc(x_{jc}, y_{jc}, k) \cdot \Delta t \cdot BR_i(k) \quad (8)$$

where $conc(x_{jc}, y_{jc}, k)$ is the pollutant concentration (μg/m3) in grid(x_{jc}, y_{jc}) at time step k, Δt is the time step, and $BR_i(k)$ denotes the breathing rate (assumed to be constant in this study) of the i-th subject exposed to the

pollutant at time step k. Breathing rates of different age groups are from the EPA *Exposure Factors Handbook* [26]. In this study, we assumed a population-wide average adult breathing rate to be 17 m^3/day. Also, we were more concerned with human exposure to NOx and particulate matter 2.5 microns or less in diameter ($PM_{2.5}$) because they are associated with a range of health risks for many population groups [27].

Case Study

To showcase the capability of the integrated modeling platform, we considered an M^3OD service scenario within an urban district and evaluated the health impact on customers under two different curbside pickup strategies: centralized and distributed.

Simulation Scenarios

We used osmWebWizard.py provided by SUMO to extract the roadway network of a target area in Riverside, California, as shown in Figure 14. This roadway network is bounded by W. Linden Street (northmost), 12th Street (southernmost), Kansas Avenue (westernmost), and Iowa Avenue (easternmost). To facilitate the generation of pedestrian demands, we further added the sidewalk for each edge in the network. To enable the dispersion modeling, we meshed the network by an 81×42 grid matrix with a grid size of 22 m. As for the vertical axis, we defined that there were three layers, which were 0.3, 0.6, and 1.2 m. In this case, for every time step, the platform could generate three (for different heights) 81×42 matrices for the concentrations of each pollutant emission.

(a) View of study network in Google Maps

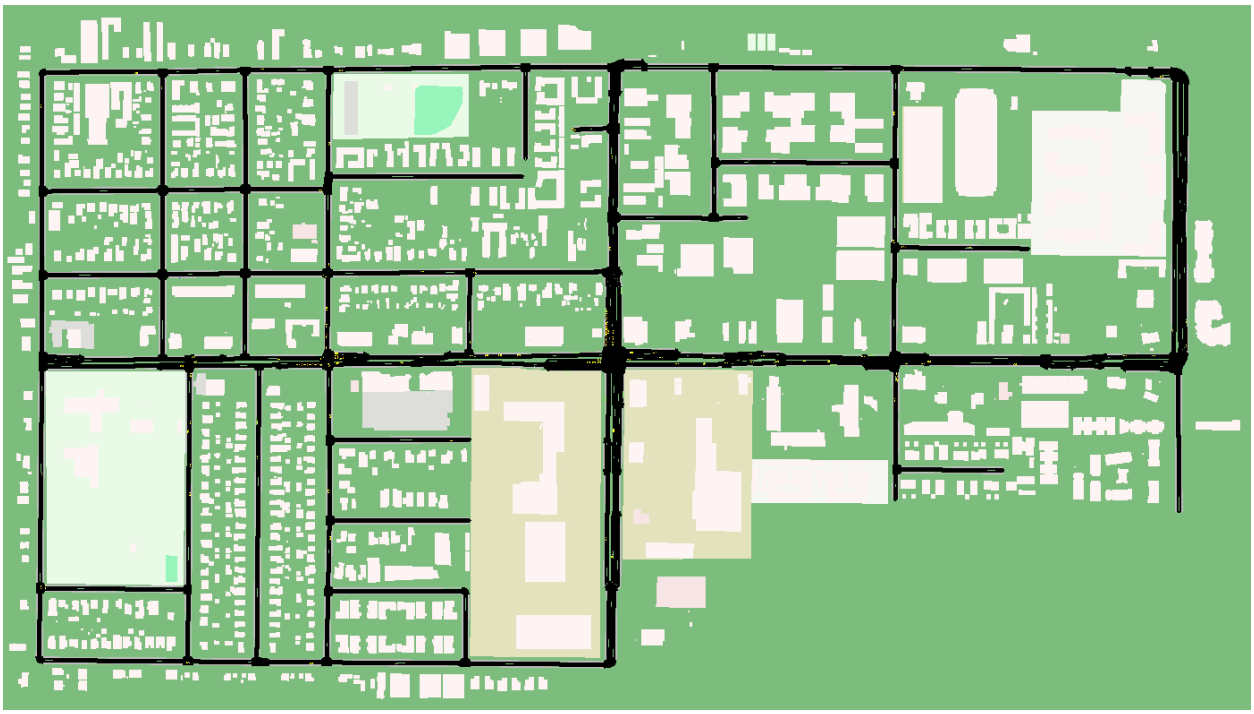

(b) View of study network in SUMO

Figure 14. Illustration of the study network.

In the simulation, we set up the vehicle mix to be 95 percent passenger vehicles and 5 percent taxis/transportation network company (TNC) vehicles. The passenger vehicles were considered background traffic, while taxis/TNC vehicles could receive pickup requests, pick up passengers at their waiting locations, and drop off passengers at their destinations. All the vehicles and pedestrians were randomly generated. Unlike the passenger vehicles, which were spawned and terminated once completing the predefined routes, SUMO provided taxis/TNC vehicles with the idling algorithm option to enable them to continue driving randomly until the next request was received. In addition, taxis/TNC vehicles could specify the drop-off durations and pickup duration, as shown in Table 2.

Table 2. Parameter Settings for Simulation Scenarios in SUMO

Vehicle Type	Taxi	Passenger Vehicle
Number	120	2,280
Minimum gap (m)	5	5
Maximum acceleration (m/s^2)	4	4
Maximum deceleration (m/s^2)	–5	–5
Length (m)	5	5
Pickup duration (s)	5	—
Drop-off duration (s)	10	—

The entire simulation length was set to 3600 seconds, and the time step was 1 second. We assumed the traffic volume per hour in this urban district was 2,400 vehicles per hour. Based on the predefined vehicle mix, the number of passenger vehicles was 2280, and the number of taxis/TNC vehicles was 120. Pedestrians also had random origins and destinations, similar to the configuration of vehicles in SUMO, but they needed to specify the locations where they should wait for pickups. Moreover, pedestrians could only access sidewalks and crossings, rather than motor roadways. Pedestrian characteristics, such as height and breathing rate, could be customized to model different groups, such as children and adults. In this study, we randomly generated only 240 adults (assuming the breathing rate to be 17 m^3/day).

To evaluate the human health impacts caused by different pickup strategies, we set up two scenarios: centralized pickup and distributed pickup. For the centralized pickup, we created a central station along one road segment, as shown in Figure 15(a), enclosed with a red box. In this scenario, all pedestrians (the blue dots) had to walk to the station and wait for pickups one by one as (shown in Figure 15[b]), and all for-service vehicles had to meet respective passengers at the same station. In the distributed pickup scenario, besides the station defined in Scenario 1, we created another seven stations as shown in Figure 15(c). Pedestrians were randomly distributed to these eight stations to wait for pickups. The wind speed was set at 2 m/second from the northwest to southeast, which is a typical meteorological condition in Riverside, California, in the summer.

(a) Centralized pickup

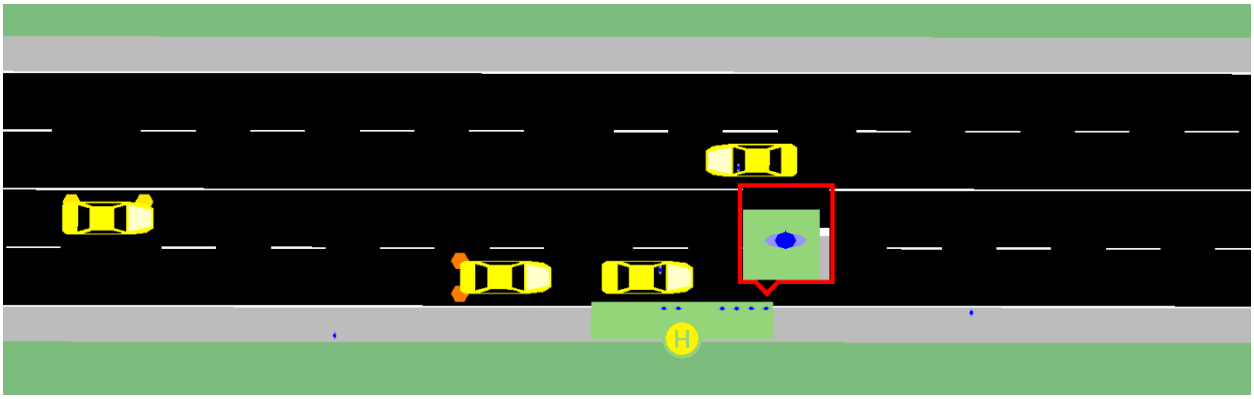

(b) Zoomed-in station in the centralized pickup scenario

(c) Distributed pickup

Figure 15. Station configuration for different curbside pickup strategies.

Result Analysis

As aforementioned, the platform could output three types of results:

- **Vehicle information.** The vehicle information log is a JSON file, including the type, location, speed, acceleration, heading, emission rate, and energy consumption rate of each individual vehicle at each time step. With post-processing, we can assess the vehicular performance in terms of safety, mobility, and environmental sustainability. This report focuses on emission results.
- **Traffic-related concentration.** The concentration log is an .npy file, which contains three (for the heights of 0.3, 0.6, and 1.2 m) 81×42 concentration matrices at each time step for each pollutant of interest. The log file can be used for further analysis or replay.
- **Pedestrian information.** This includes the demographic characteristics (e.g., child/adult), location, speed, and exposure of each individual pedestrian at each time step. The output file can be used to evaluate the quality of M^3OD services (e.g., waiting time) and assess human exposure to the pollutants of interest either individually or in an aggregated manner.

Vehicular Emission

Table 3 compares the emission results between two pickup strategies. As the table shows, the total emission of CO_2, NOx, and $PM_{2.5}$ for the distributed pickup scenario are slightly higher than those of the centralized pickup scenario. This is mainly due to the increase of vehicle miles traveled (VMT). After normalization by the distance, there is no significant difference in the total emission factor (i.e., total emission/VMT) between the two strategies, ranging from –0.7 to –1.2 percent.

Table 3. Vehicular Emission Comparison for Different Pickup Strategies

Scenario		Centralized	Distributed	Difference
Vehicle miles traveled (VMT)		2,801	2,879	2.8%
Total emission of passenger vehicles (g)	CO_2	1,218,631.81	1,219,444.46	0.07%
Total emission of taxis (g)		763,804.53	795,052.61	4%
Total emission (g)		1,982,436.34	2,014,497.08	1.6%
Total emission/VMT (g/mile)		707.70	699.59	–1.2%
Total emission of passenger vehicles (g)	NOx	243.54	244.16	0.3%
Total emission of taxis (g)		138.60	145.33	0.5%
Total emission (g)		382.15	389.48	1.9%
Total emission/VMT (g/mile)		0.13642	0.1352	–0.9%
Total emission of passenger vehicles (g)	$PM_{2.5}$	2.20	2.20	0%
Total emission of taxis (g)		1.43	1.50	4.9%
Total emission (g)		3.63	3.71	2.2%
Total emission/VMT (g/mile)		0.001296	0.001287	–0.7%

Network-Wise Grid-Based Concentration

To present the difference in traffic-related concentration, we compared the estimated concentration profiles of both NOx and $PM_{2.5}$ (over time) under two pickup scenarios at the location of the bus station. As shown in Figure 16, most of the time, the concentrations at the bus station when applying the centralized pickup strategy were higher than those of the distributed scenario. The mean concentrations of NOx and $PM_{2.5}$ across time of the centralized pickup strategy were 16 and 52 percent, respectively, higher than the values of the distributed pickup strategy.

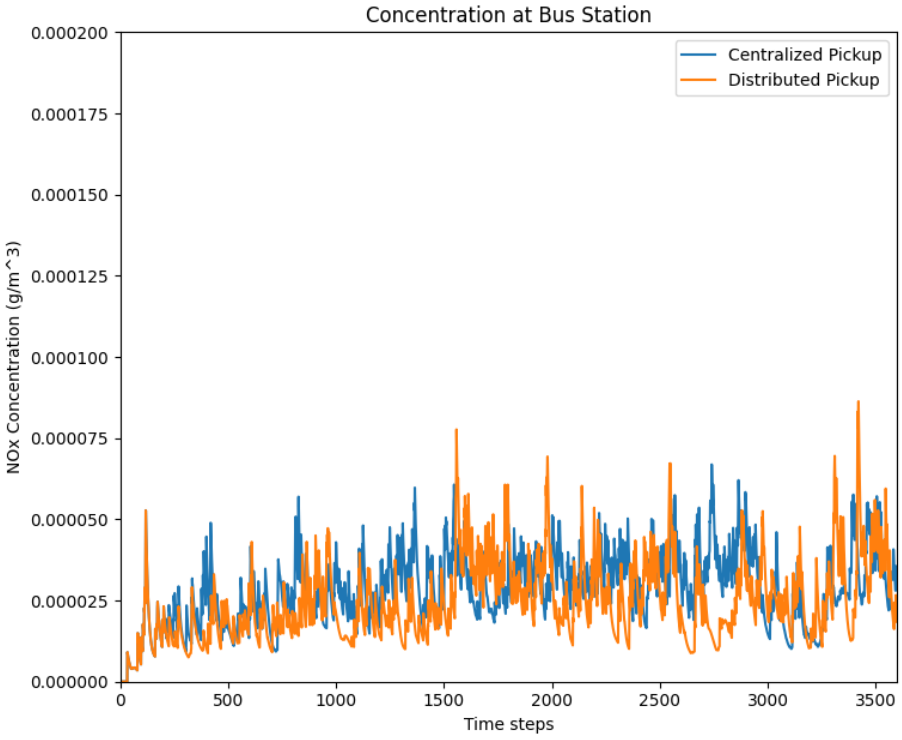

(a) NOx concentration profile

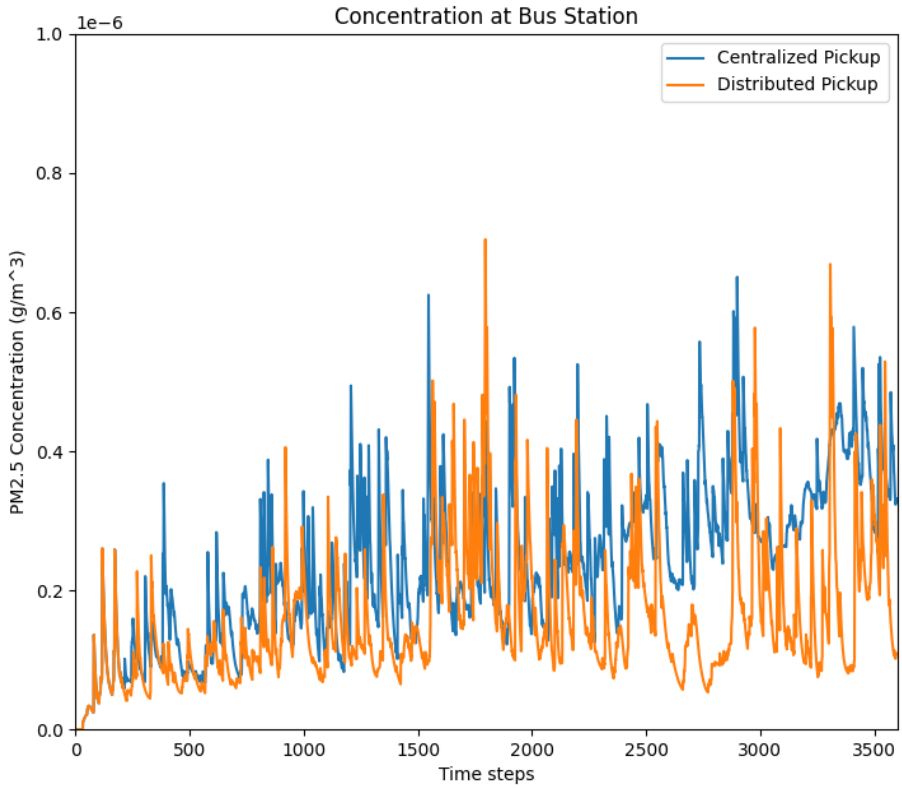

(b) $PM_{2.5}$ concentration profile

Figure 16. Comparison of pollutant concentration profiles between two pickup scenarios at the central station.

Furthermore, Figure 17 shows a typical screenshot of the network-wise concentration difference of both NOx and $PM_{2.5}$ between two pickup strategies (i.e., $conc_{central} - conc_{distributed}$). As the figure shows, the largest difference in concentration between these two strategies occurs at or around the location of the central station.

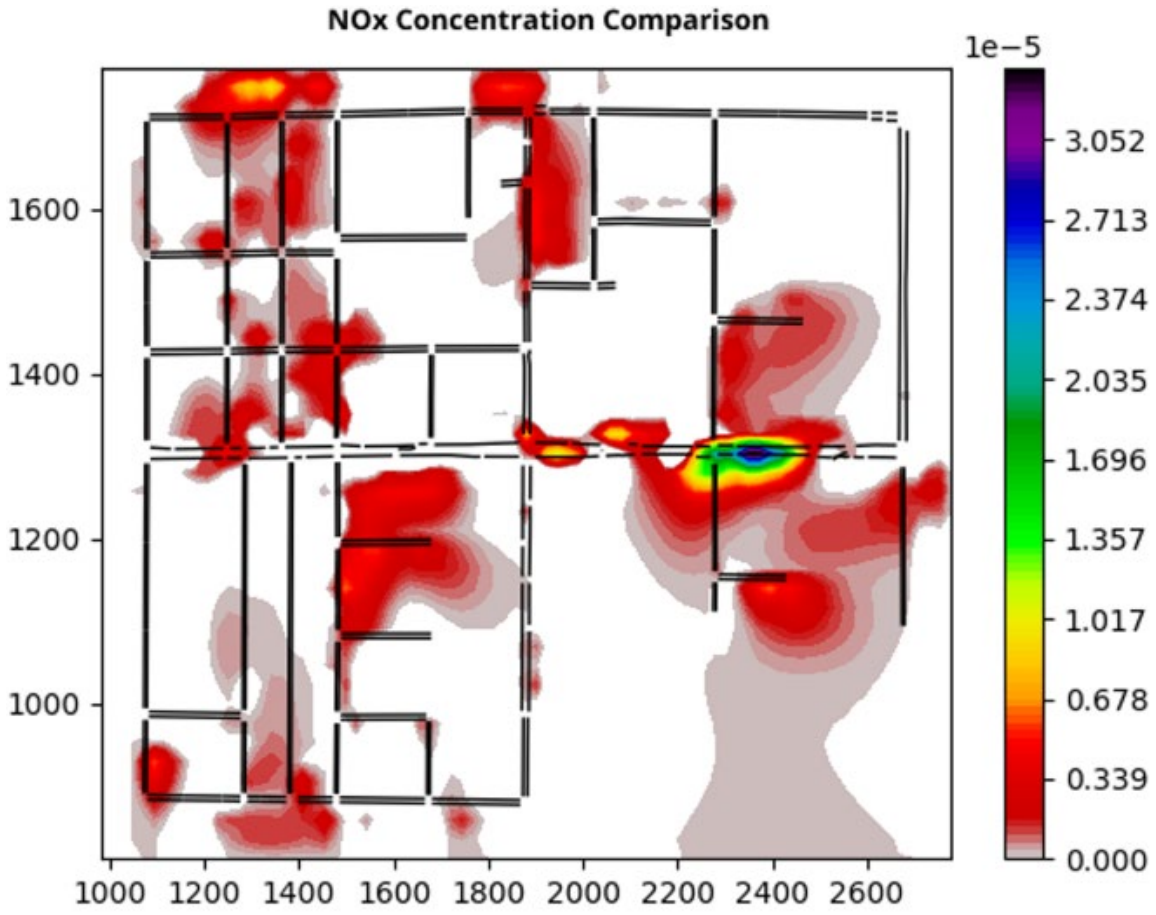

(a) NOx results

(b)

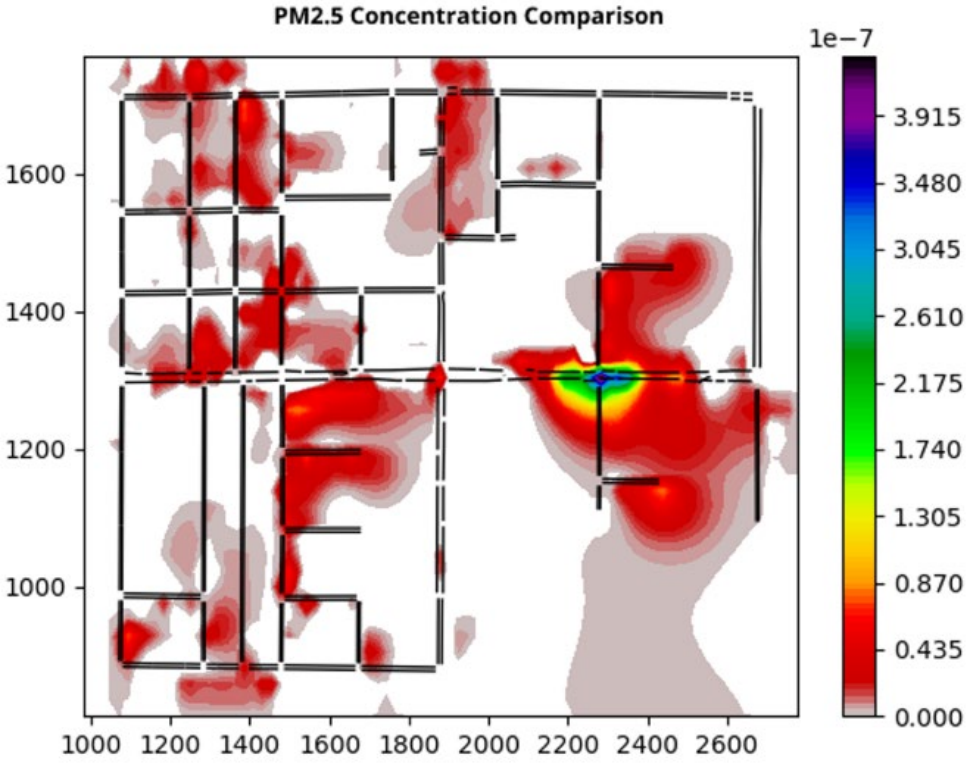

(b) $PM_{2.5}$ results

Figure 17. Difference of network-wise pollutant concentration between the centralized scenario and the distributed scenario.

Pollutant Exposure

This study focused on the pedestrian exposure to NOx and $PM_{2.5}$. Figure 18(a) and Figure 18(b) show the accumulative inhale mass (AIM) of NOx over time for each individual pedestrian (represented by each curve) under centralized and distributed pickup strategies, respectively. Figure 19 presents similar results for the AIM (over time) of $PM_{2.5}$. The pedestrian's AIM of pollutants in the centralized scenario are much higher than that in the distributed scenario. Besides the potentially higher concentrations of pollutants, another reason is that pedestrians spend more time waiting for pickup in the centralized scenario.

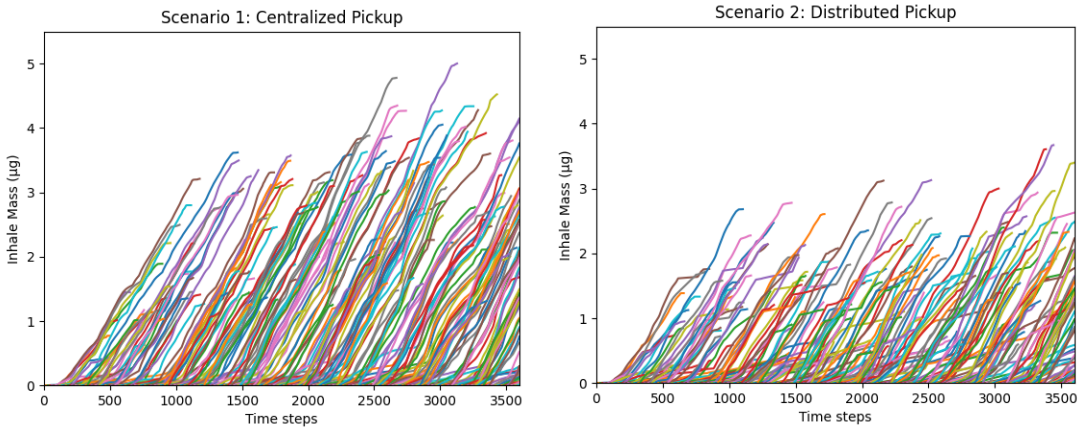

(a) Centralized pickup (b) Distributed pickup

Figure 18. Pedestrian AIM of NOx over time under different pickup scenarios (each curve representing one human subject).

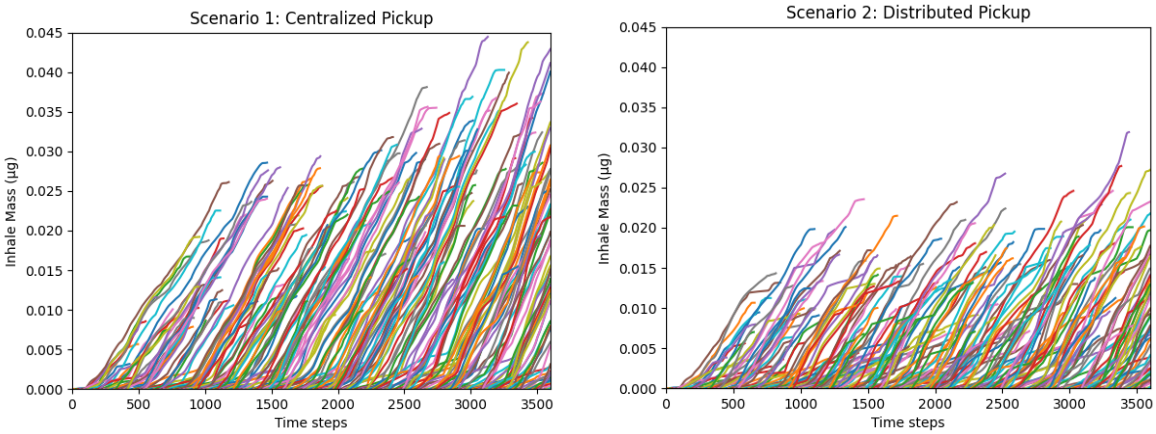

(a) Centralized pickup (b) Distributed pickup

Figure 19. Pedestrian AIM of $PM_{2.5}$ over time under different pickup scenarios (each curve representing one human subject).

Table 4 summarizes the key statistics (i.e., maximum, median, and mean) of the distributions of pedestrian AIM of NOx and $PM_{2.5}$. For NOx, the maximum AIM in the centralized scenario is 5 µg, which is 36 percent more than that in the second scenario. The median AIM and mean AIM in the centralized scenario are 82 and 70 percent, respectively, higher than those in the distributed scenario. For $PM_{2.5}$, the maximum AIM when applying the centralized pickup strategy is 38 percent higher than that of the distributed strategy. The median AIM and mean AIM in the distributed scenarios are both 0.011 µg, which is much lower than the values of the centralized scenario.

Table 4. Comparison of Human Exposure to NOx and $PM_{2.5}$ with Different Pickup Strategies

Scenario		Centralized	Distributed	Difference
Total number of pedestrians	NOx	240	240	—
Maximum inhale mass (μg)		5.00	3.67	36%
Minimum inhale mass (μg)		0	0	0%
Median inhale mass (μg)		2.27	1.25	82%
Average inhale mass (μg)		2.23	1.31	70%
Total number of pedestrians	$PM_{2.5}$	240	240	0%
Maximum inhale mass (μg)		0.044	0.032	38%
Minimum inhale mass (μg)		0	0	0%
Median inhale mass (μg)		0.021	0.011	91%
Average inhale mass (μg)		0.020	0.011	82%

Conclusions and Recommendations

This study proposed an integrated analysis, modeling, and simulation platform for estimating traffic-related health impacts in a microscopic manner. Besides the traffic model and emission models, we introduced a grid-based concentration model and a human exposure model as the key components of this platform. A case study on the evaluation of different curbside management strategies showed the effectiveness of the developed tool. The centralized pickup strategy has a great significant negative effect on subject health in terms of exposure to NOx and $PM_{2.5}$, compared to distributed pickup strategy. The difference in AIM per person on average can be as high as 70 and 82 percent for NOx and $PM_{2.5}$, respectively. The reasons may include relatively higher concentration due to the bottleneck created by the for-service vehicles and longer waiting time for pedestrians in the centralized pickup scenario.

In the future, we will apply this tool to investigate the health impacts of different roadway design and transportation systems management and operations strategies. In addition, we will conduct more sophisticated field experiments to collect data for dispersion model calibration, and will keep improving the model fidelity by considering more realistic aerodynamic effects (e.g., turbulence) in the field of transportation.

Research Outputs, Outcomes, and Impacts

We completed two draft papers summarizing the major efforts and findings from this study.

- Ding, Y., Zhao, X., Luo, J., Wu, G., and Venkatram, A. Field Study to Estimate Exposure to Vehicle Exhaust during Idling and Starting (submitted).
- Zhao, X., Wu, G., Hao, P., Venkatram, A., Luo, J., Hu, S., and Boriboonsomsin, K. Quantifying the Environmental and Health Impacts of Curbside Management Using an Integrated Simulation Platform (to be submitted).

Technology Transfer Outputs, Outcomes, and Impacts

This project produced the following technology transfer outputs, outcomes, and impacts:

- **Experimental data sets.** The data sets include data collected in the field experiments over two days. The data sets include meteorological data, emission data, and fuel consumption data. https://drive.google.com/drive/folders/1bda_n6GT9uB59HzFScRAOhQA-x_8kSaC?usp=sharing

- **Code developed for dispersion modeling (MATLAB version).** The code was developed for a simple version of the proposed dispersion model, which has only a limited number of vehicles (pollutant sources).
  https://github.com/XuanpengZhao/CARTEEH-2021/tree/main/DispersionModel/Matlab
- **Code developed for dispersion modeling (Python version).** The code was developed for the main proposed dispersion model system.
  https://github.com/XuanpengZhao/CARTEEH-2021/tree/main/DispersionModel/Python
- **Dispersion model output sample data sets.** The data sets include a sample output of the proposed dispersion model.
  https://drive.google.com/drive/folders/1m4B4AVQiXanYOIPlSJ5CBQi_CGKjb4GI?usp=sharing

Education and Workforce Development Outputs, Outcomes, and Impacts

This study is considered as a multidisciplinary collaboration in which graduate students from the Departments of Electrical and Computer Engineering (ECE) and Mechanical Engineering (ME) were involved. More specifically:

- Xuanpeng Zhao, a second-year Ph.D. student in the ECE Department, focused on developing the numerical dispersion model, coding the integrated platform based on SUMO and its APIs, and building a MATLAB-based GUI for displaying the pollutant concentration results in an online manner.
- Yifan Ding, a fourth-year Ph.D. student in the ME Department, provided the access to anemometers, helped collect field data for dispersion model development, and contributed to the puff model development.

References

1. U.S. Environmental Protection Agency. Inventory of U.S. Greenhouse Gas Emissions and Sinks: 1990–2018. EPA 430-R-20-002, April 2020.

2. Sperling, D. (2018). Three Revolutions: Steering Automated, Shared, and Electric Vehicles to a Better Future. Island Press.

3. Wang, Z., Liao, X., Zhao, X., Han, K., Tiwari, P., Barth, M. J., and Wu, G. (2020, May). A Digital Twin Paradigm: Vehicle-to-Cloud Based Advanced Driver Assistance Systems. *2020 IEEE 91st Vehicular Technology Conference (VTC2020-Spring)*, pp. 1–6.

4. Altan, O. D., Wu, G., Barth, M. J., Boriboonsomsin, K., and Stark, J. A. (2017). GlidePath: Eco-Friendly Automated Approach and Departure at Signalized Intersections. *IEEE Transactions on Intelligent Vehicles*, 2(4), 266–277.

5. Katsaros, K., Kernchen, R., Dianati, M., and Rieck, D. (2011, July). Performance Study of a Green Light Optimized Speed Advisory (GLOSA) Application Using an Integrated Cooperative ITS Simulation Platform. *2011 7th International Wireless Communications and Mobile Computing Conference,* pp. 918–923.

6. Lee, J., and Park, B. (2012). Development and Evaluation of a Cooperative Vehicle Intersection Control Algorithm under the Connected Vehicles Environment. *IEEE Transactions on Intelligent Transportation Systems,* 13(1), 81–90.

7. Fellendorf, M., and Vortisch, P. (2010). *Microscopic Traffic Flow Simulator VISSIM. Fundamentals of Traffic Simulation*, Springer, New York, NY, pp. 63–93.

8. Aimsun. *Aimsun Next 20 User's Manual*. Aimsun Next Version 20.0.3, Barcelona, Spain.

9. Behrisch, M., Bieker, L., Erdmann, J., and Krajzewicz, D. (2011). SUMO–Simulation of Urban Mobility: An Overview. *Proceedings of SIMUL 2011, The Third International Conference on Advances in System Simulation*, ThinkMind.

10. Krajzewicz, D., Erdmann, J., Behrisch, M., and Bieker, L. (2012). Recent Development and Applications of SUMO—Simulation of Urban Mobility. *International Journal on Advances in Systems and Measurements*, 5(3&4).

11. Scora, G., and Barth, M. (2006). *Comprehensive Modal Emissions Model (CMEM), Version 3.01, User Guide.* Centre for Environmental Research and Technology, University of California, Riverside.

12. Rakha, H., Ahn, K., and Trani, A. (2004). Development of VT-Micro Model for Estimating Hot Stabilized Light Duty Vehicle and Truck Emissions. *Transportation Research Part D: Transport and Environment*, 9(1), 49–74.

13. Keller, M., Hausberger, S., Matzer, C., Wüthrich, P., and Notter, B. (2010). *Handbook of Emission Factors for Road Transport (HBEFA) 3.1.* Technical Report, quick reference, INFRAS.

14. U.S. Environmental Protection Agency. (2009, December). *EPA Releases MOVES2010 Mobile Source Emissions Model: Questions and Answers.* EPA-420-F-09-073.

15. Holmes, N. S., and Morawska, L. (2006). A Review of Dispersion Modelling and Its Application to the Dispersion of Particles: An Overview of Different Dispersion Models Available. *Atmospheric Environment*, 40(30), 5902–5928.

16. Brode, R. W., and Anderson, B. (2008). *Technical Issues Related to CALPUFF Near-Field Applications.* U.S. Environmental Protection Agency.

17. Paine, R. J., Brode, R. W., Wilson, R. B., Cimorelli, A. J., Perry, G. S., Weil, J. C., ... and Lee, R. F. (2003). AERMOD: Latest Features and Evaluation Results. *Proceedings of the 96th Air and Waste Management Association Annual Conference and Exhibition,* Paper No. 69878, pp. 22–26.

18. Lefebvre, W., Van Poppel, M., Maiheu, B., Janssen, S., and Dons, E. (2013). Evaluation of the RIO-IFDM-Street Canyon Model Chain. *Atmospheric Environment*, 77, 325–337.

19. Shi, T., Ming, T., Wu, Y., Peng, C., and Fang, Y. (2020). The Effect of Exhaust Emissions from a Group of Moving Vehicles on Pollutant Dispersion in the Street Canyons. *Building and Environment*, 181, 107120.

20. Damoiseaux, M., and De Schutter, B. (2021, September). An Efficient Dispersion Model for Control of Emission Levels in the Vicinity of Freeways. *2021 IEEE International Intelligent Transportation Systems Conference*, pp. 2455–2462.

21. Zegeye, S. K. (2011). *Model-Based Traffic Control for Sustainable Mobility*.

22. U.S. Environmental Protection Agency (2010). *MOVES2010 Highway Vehicle Population and Activity Data*. EPA-420-R-10-026.

23. Wang, Z., Wu, G., and Scora, G. (2020). *MOVESTAR: An Open-Source Vehicle Fuel and Emission Model Based on USEPA MOVES.* arXiv preprint arXiv:2008.04986.

24. Ding, Y. *et al.* (2023) Field study to estimate exposure to vehicle exhaust during idling and starting, *Atmospheric Pollution Research*, 14(1), p. 101632.

25. Bennett, D. H., McKone, T. E., Evans, J. S., Nazaroff, W. W., Margni, M. D., Jolliet, O., and Smith, K. R. (2002). Defining Intake Fraction. *Environmental Science and Technology*, 36(9).

26. U.S. Environmental Protection Agency. (2011). *Exposure Factors Handbook: 2011 Edition*. EPA/600/R-09/052F, Office of Research and Development. Available at https://www.epa.gov/expobox/exposure-factors-handbook-2011-edition.

27. Weichenthal, S., Kulka, R., Bélisle, P., Joseph, L., Dubeau, A., Martin, C., ... and Dales, R. (2012). Personal Exposure to Specific Volatile Organic Compounds and Acute Changes in Lung Function and Heart Rate Variability among Urban Cyclists. *Environmental Research*, 118, 118–123.